A mixed approach for studying size effects and connecting interactions of planar nano structures as resonant mass sensors

S. K. Jalali[a,b], M. H. Naei[a], N. M. Pugno[b,c,d]

[a]*School of Mechanical Engineering, University of Tehran, Tehran, Iran*

[b]*Laboratory of Bio-Inspired and Graphene Nanomechanics, Department of Civil, Environmental and Mechanical Engineering, Università di Trento, via Mesiano, 77, 38123 Trento, Italy*

[c]*Center for Materials and Microsystems, Fondazione Bruno Kessler—via Sommarive 18, 38123, Povo, Povo (Trento), Italy*

[d]*School of Engineering and Materials Science, Queen Mary University of London, Mile End Road, London E1 4NS, UK*

Abstract

Present paper investigates the potential application of planar nano structures with attached nano particles as nano resonant sensors by introducing a nonlocal plate model which considers size effects. To take into account an elastic connection between the nano plate and the attached nanoparticle, the nano particle is considered as a mass-spring system. Then, a mixed approach based on pseudo-spectral and integral quadrature rule is implemented to numerically determine the frequency shift caused by the attached mass-spring system. Obtained results are in a good agreement with those available in the literature which reveals that the proposed combined method provides accurate results for structural problems with concentrated objects. Results show that for soft connections with small values of spring constant the predicted frequency shift is greater than rigid connections. It means that considering a rigid connection instead of elastic one will underestimate the frequency shift of nano resonant sensors. Also, it is shown that neglecting size effects results in overestimating the frequency shift of nano resonant sensors. Furthermore, nano plates with greater aspect ratios offer smaller dimensionless frequency shifts and the maximum belongs to a square one. The presented results could be useful as a guideline for designing nano resonant sensors of plane shapes like graphene based mass sensors.

1. Introduction

In recent years, nano structures as new members in structural mechanics have received a notable attraction due to their wide application in nano technology and therefore prediction of response of these elements against various mechanical loading situations like vibration, buckling, bending, and etc. is prominent in designing of future nano scale devices and structures. Reviewing the literature, modeling of nano sized structures is mainly conducted based on four main approaches: (I) molecular dynamics (MD) (Ansari et al. 2012; Xiang and Shen 2014), (II) molecular structural mechanics (Sakhaee-Pour 2009; Wang et al. 2013), (III) local (classical) continuum elasticity (Liew et al. 2006; Behfar and Naghdabadi 2005), (IV) nonlocal elasticity (Zenkour and Abouelregal 2014; Jomehzadeh et al. 2012). The computational expense for the first two approaches is directly related to the size of the studied system, as they consider all constitutive particles of the nano structure. Hence, their application is limited to a restricted size of nano structures. Instead, both local and nonlocal approaches are able to model nano structures without any restriction in the number of consisting particles, thanks to their continuum method of modeling. In the continuum view, based on the geometry and the mechanical properties, nano structures are usually considered as known structural

elements like beams, plates and shells and their mechanical behavior is analyzed using related well-known theories.

Although the local (classical) continuum elasticity may make a desirable insight about the behavior of nano structures, however, due to neglecting the structural discreteness the obtained results are not realistic enough. This limitation overcomes in nonlocal version of continuum elasticity (Eringen 1983) with introducing small scale effects. Reports reveal that the results obtained by nonlocal model with a proper small scale parameter are in good agreement with those obtained by atomistic approaches. A review on the application of nonlocal elasticity in modeling of carbon based nano structures could be found in the work by Arash and Wang (2012).

Nano structures are main candidates for nano sensing applications because of their proper sizes and superior mechanical and electrical properties (Angione et al. 2014). Resonant sensors are a group of nano sensors which detect nano particles in a dynamic mode from a vibration analysis. The main idea for detecting attached particles is to measure the resonant frequency shift of the sensor caused by changes in total mass of the system. Potential application of carbon based nano structures like Fullerene and Carbon nanotubes as resonant mass sensors are widely investigated (Giannopoulos 2014; Joshi et al. 2010; Mehdipour et al. 2011). Recently, graphene, the thinnest two-dimensional flat structure consisting of carbon atoms settled in a hexagonal lattice, is taken into consideration in resonant sensing application due to its remarkable sensing privilege like large surface area and high bending flexibility. Therefore, vibration analysis of graphene sheets with attached masses is a significant issue in the field and has been studied in both continuum and atomistic approaches.

In continuum approaches, a graphene based nano resonant sensor is usually considered as a nano plate with attached masses. Murmu and Adhikari (2013) proposed a nonlocal mass sensor model using vibrating monolayer cantilever graphene sheets and analytical solution were derived for the frequency shift due to the added mass. Adhikari and Chowdhury (2012) also investigated the possibility of implementing graphene sheets as nano resonant sensors based on local elasticity. The potential application of single-layered graphene sheets as nano mass sensors based on nonlocal Kirchhoff plate theory and Galerkin method was studied by Shen et al. (2012) studied and influence of the mass value and position on the frequency shift were discussed. As a similar work, Zhou et al. (2014) analyzed a circular graphene sheet carrying a nano particle as a nano resonant mass sensor. Lee et al. (2013a) applying nonlocal elasticity considered the graphene sheet as a rectangular nano plate with an attached mass and equations of motion are analytically solved for simply supported boundary conditions and effects of the small scale effect and aspect ratio on sensitivity of sensor were studied in detail.

In Atomistic view, both MD and molecular structural mechanics have also been implemented by researchers for modeling of nano resonant sensors. Arash et al. (2011) investigated the potential application of single-layered graphene sheets in detection of noble gases was by applying MD simulations. Sakhaee-Pour et al. (2008) applied finite element molecular structural mechanics to model the vibrational behavior of single-layered graphene sheets and investigated the effect of point mass on the fundamental frequencies for mass sensing applications. Lee et al. (2013b) studied single layered graphene mass resonant sensors with various boundary conditions by using finite element molecular structural mechanics and influence of value and position of attached mass and boundary conditions on the sensitivity of sensor was explored. Jalali et al. (2014) studied the application of graphene sheets as resonant sensors in detection of ultra-fine nanoparticles via both MD and nonlocal elasticity approaches. To take into consideration the effect of geometric nonlinearity, nonlocality, and atomic interactions between graphene and nanoparticles, a nonlinear nonlocal plate model carrying an attached mass-spring system is introduced. Nonlocal small scale parameter is calibrated by matching frequency shifts obtained by nonlocal and MD simulation approaches with same vibration amplitude.

Reviewing the literature reveals that analysis of frequency characteristics of nano structures and especially nano plates is a consequential issue for designing future ultra-sensitive nano sensors. This paper aims to propose a nano plate model with an attached mass for vibration analysis of resonant mass sensors, in the framework of nonlocal continuum elasticity. However, with regard to the previous researches, it can be concluded that the influence of interaction between the attached mass and the sensor has not been reported. Therefore, in present work this interaction has taken into account by considering a mass-spring system as the attached nano particle. Also a pseudo-spectral procedure in conjunction with integration quadrature (IQ) method is introduced to numerically solve the problem. Influence of small scale parameter, value and position of the attached mass, spring constant, aspect ratio, thickness to side ratio and boundary conditions on frequency characteristics of these sensors will be discussed in detail.

2. Nonlocal shear deformation nano plate model

Consider a rectangular nano plate of length a, width b, the effective thickness h and mass density ρ with a mass-spring system (M0, K0) mounted on an arbitrary position (x0,y0) of the plate as shown in Fig. 1. The origin of the Cartesian coordinates system (x,y,z) lies on the corner of the mid-plane. Displacement components U, V, W, ϕx and ϕy define displacements in x, y and z directions and the rotation about the y and x axis, respectively. To take into consideration shear deformation effects especially for nano plates with large thickness to length size ratios, the first order shear deformation plate theory (FSDT) is applied to the model as follows.

$$U(x,y,z,t) = z\varphi_x(x,y,t) \tag{1a}$$

$$V(x,y,z,t) = z\varphi_y(x,y,t) \tag{1b}$$

$$W(x,y,z,t) = w_0(x,y,t) \tag{1c}$$

where w0 is the mid-plane displacement components along z directions and t defines time. The linear strain–displacement relations are (Reddy 2003):

$$\varepsilon_x = z\varphi_{x,x} \tag{2a}$$

$$\varepsilon_y = z\varphi_{y,y} \tag{2b}$$

$$\gamma_{xy} = z\left(\varphi_{x,y} + \varphi_{y,x}\right) \tag{2c}$$

$$\gamma_{xz} = \varphi_x + w_{0,x} \tag{2d}$$

$$\gamma_{zy} = \varphi_y + w_{0,y} \tag{2e}$$

where (),x and (),y indicate the differentiation with respect to x and y, respectively.

The small scale effect of nonlocal continuum elasticity appears in constitutive stress–strain relations. Based on the known local (classical) elasticity, stress at a point depends only on the strain at that point and the local stress tensor t at a point is related to the strain tensor ε at that point by the generalized Hooke's law as follows:

$$\boldsymbol{t} : \boldsymbol{C} : \varepsilon \tag{3}$$

where C is the fourth-order elasticity tensor (Reddy 2008). However, according to nonlocal elasticity of Eringen (2002), the stress at a point is related on the strain at the every point of the continuum domain through an integration on the whole elastic body. Eringen (1983) showed that the integral form of constitutive relations can be written in an equivalent simpler differential form as follows.

$$\left(1-\mu\nabla^2\right)\boldsymbol{\sigma}:\boldsymbol{C}:\varepsilon,\quad \mu=(e_0a_0)^2 \tag{4}$$

In which μ is the nonlocal parameter, e0 is a material constant, a0 is the internal characteristic length, ∇2 is the two-dimensional Laplace operator, and σ is the nonlocal stress tensor. The nonlocal version of elasticity is able to consider discontinuities in the elastic medium by considering small scale parameter opposed to zero. The nonlocal form of stress–strain relationship for the plane stress state of nano plates can be explained as:

$$\begin{Bmatrix}\sigma_x\\ \sigma_y\\ \tau_{zy}\\ \tau_{xz}\\ \tau_{xy}\end{Bmatrix}-\mu\nabla^2\begin{Bmatrix}\sigma_x\\ \sigma_y\\ \tau_{zy}\\ \tau_{xz}\\ \tau_{xy}\end{Bmatrix}=\begin{bmatrix}\bar{Q} & \nu\bar{Q} & 0 & 0 & 0\\ \nu\bar{Q} & \bar{Q} & 0 & 0 & 0\\ 0 & 0 & G & 0 & 0\\ 0 & 0 & 0 & G & 0\\ 0 & 0 & 0 & 0 & G\end{bmatrix}\begin{Bmatrix}\varepsilon_x\\ \varepsilon_y\\ \gamma_{zy}\\ \gamma_{xz}\\ \gamma_{xy}\end{Bmatrix}$$
$$\bar{Q}=\frac{E}{\left(1-\nu^2\right)},\quad G=\frac{E}{2(1+\nu)} \tag{5}$$

E, v and G are Young's modulus, Shear modulus and Poison's ratio of the nano plates, respectively. The nonlocal force and moment resultants can be calculated by integrating stress components across the plate thickness.

$$M=\left[M_{xx},M_{yy},M_{xy}\right]^T=\int_{-h/2}^{h/2}\left[\sigma_{xx},\sigma_{yy},\sigma_{xy}\right]^T z\,dz \tag{6a}$$

$$Q=\left[Q_x,Q_y\right]^T=K_s\int_{-h/2}^{h/2}\left[\tau_{xz},\tau_{zy}\right]^T dz \tag{6b}$$

where Ks is the shear correction coefficient set to 5/6 (Reddy 2003). Considering Eqs. (5) and (6a, 6b) one can obtain:

$$\begin{Bmatrix}M_{xx}\\ M_{yy}\\ M_{xy}\end{Bmatrix}-\mu\nabla^2\begin{Bmatrix}M_{xx}\\ M_{yy}\\ M_{xy}\end{Bmatrix}=\begin{bmatrix}D & \nu D & 0\\ \nu D & D & 0\\ 0 & 0 & \frac{D(1-\nu)}{2}\end{bmatrix}\begin{Bmatrix}\varphi_{x,x}\\ \varphi_{y,y}\\ \varphi_{x,y}+\varphi_{y,x}\end{Bmatrix},D=\frac{Eh^3}{12\left(1-\nu^2\right)} \tag{7a}$$

$$\begin{Bmatrix}Q_x\\ Q_y\end{Bmatrix}-\mu\nabla^2\begin{Bmatrix}Q_x\\ Q_y\end{Bmatrix}=K_s\begin{bmatrix}\frac{A(1-\nu)}{2} & 0\\ 0 & \frac{A(1-\nu)}{2}\end{bmatrix}\begin{Bmatrix}\gamma_{xz}\\ \gamma_{zy}\end{Bmatrix},A=\frac{Eh}{\left(1-\nu^2\right)} \tag{7b}$$

where A and D are the longitudinal and flexural rigidity of the nano plate, respectively.

The governing equations of motion for free vibration of a shear deformable plate carrying a mass-spring system can be obtained by using stationary potential energy method as follows (Reddy 2003):

$$Q_{x,x}+Q_{y,y}+K_0\left[z_0-w_0(x_0,y_0)\right]\delta(x-x_0)\delta(y-y_0)=I_0\,\ddot{w}_0 \tag{8a}$$

$$M_{xx,x}+M_{xy,y}-Q_x=I_2\ddot{\varphi}_x \tag{8b}$$

$$M_{yy,y}+M_{xy,x}-Q_y=I_2\ddot{\varphi}_y \tag{8c}$$

$$K_0\left[w_0(x_0,y_0)-z_0\right]=M_0\ddot{z}_0 \tag{8d}$$

where dot operator indicate differentiation with respect to t and I0 and I2 are mass moments of inertia which are defined as follows:

$$(I_0, I_2) = \int_{-h/2}^{h/2} \rho\left(1, z^2\right) dz \tag{8e}$$

Also, the Dirac Delta function, given in Eq. (8a), is defined as:

$$\delta(x - x_0) = 0, x \neq x_0$$
$$\int_0^{\infty} f(x)\delta(x - x_0)dx = \int_0^{a} f(x)\delta(x - x_0)dx = f(x_0), x < a \tag{8f}$$

Substituting Eqs. (7a, b) in Eq. (8a, b, c) gives the nonlocal equations of motion in terms of the displacement components:

$$\begin{aligned} &K_s A \frac{(1-\nu)}{2}\left(w_{0,xx} + w_{0,yy} + \varphi_{x,x} + \varphi_{y,y}\right) \\ &\quad + K_0\left[z_0 - w_0(x_0, y_0)\right]\delta(x - x_0)\delta(y - y_0) \\ &= I_0\left(\ddot{w}_0 - \mu\,\ddot{w}_{0,xx} - \mu\,\ddot{w}_{0,yy}\right) \end{aligned} \tag{9a}$$

$$\begin{aligned} &D\left[\varphi_{x,xx} + \nu\varphi_{y,xy} + \frac{1-\nu}{2}\left(\varphi_{x,yy} + \varphi_{y,xy}\right)\right] \\ &\quad - K_s A \frac{(1-\nu)}{2}\left(\varphi_x + w_{0,x}\right) \\ &= I_2\left(\ddot{\varphi}_x - \mu\,\ddot{\varphi}_{x,xx} - \mu\,\ddot{\varphi}_{x,yy}\right) \end{aligned} \tag{9b}$$

$$\begin{aligned} &D\left[\varphi_{y,yy} + \nu\varphi_{x,xy} + \frac{1-\nu}{2}\left(\varphi_{y,xx} + \varphi_{x,xy}\right)\right] \\ &\quad - K_s A \frac{(1-\nu)}{2}\left(\varphi_y + w_{0,y}\right) \\ &= I_2\left(\ddot{\varphi}_y - \mu\,\ddot{\varphi}_{y,xx} - \mu\,\ddot{\varphi}_{y,yy}\right) \end{aligned} \tag{9c}$$

$$K_0\left[w_0(x_0, y_0) - z_0\right] = M_0\ddot{z}_0 \tag{9d}$$

Equation (9a) is singular at the point (x0, y0) where the mass-spring system is located. However, considering Eq. (8f) one can integrate Eq. (9a) as follows:

$$\begin{aligned} &\int_0^a \int_0^b \left\{K_s A \frac{(1-\nu)}{2}\left(w_{0,xx} + w_{0,yy} + \varphi_{x,x} + \varphi_{y,y}\right)\right. \\ &\quad \left. -I_0\left(\ddot{w}_0 - \mu\,\ddot{w}_{0,xx} - \mu\,\ddot{w}_{0,yy}\right)\right\} dxdy = K_0\left[w_0(x_0, y_0) - z_0\right] \end{aligned} \tag{9e}$$

This integration form will be used in the next section for solution procedure. For a nanoplate problem it is theoretically possible to consider either clamped or simply supported boundary conditions as follows:

Clamped (CCCC):

$$Alledges : w_0 = 0, \varphi_x = 0, \varphi_y = 0 \tag{10a}$$

Simply Supported (SSSS):

$$\begin{aligned} &Atx = 0, a : w_0 = 0, \varphi_y = 0, \varphi_{x,x} = 0 \\ &Aty = 0, b : w_0 = 0, \varphi_x = 0, \varphi_{y,y} = 0 \end{aligned} \tag{10b}$$

In the result section we will consider both these boundaries for the purpose of generality. However, it should be noted that for graphene sheets as the main candidate for planar nano resonant sensors, carbon atoms next to the boundaries can easily move in transverse direction and the slope of deformed SLGSs next to the boundaries is considerable during vibration. Accordingly, for graphene based sensors it is recommended to address the results obtained by considering simply supported boundary conditions.

In the next section, this set of partial differential equations will be numerically solved as an eigenvalue problem in order to determine the frequency response of the nano plate with attached mass.

3. Pseudo-spectral solution procedure

The spectral method as a powerful numerical technique has been widely applied to scientific problems (Boyd 2000). Usually, for the non-periodic finite domains like plates, the collocation version of spectral method called the pseudo-spectral method with use of Chebyshev polynomials as the basis function could be the best choice (Jalali et al. 2010; Jalali et al. 2011). The basic idea in this method is to approximate the derivative of an unknown function, F, at a collocation point by an equivalent weighted linear sum of the function values at all collocation points. In one-dimensional domains it is explained as follows:

$$\begin{aligned} F_{,x}^{(n)}(x_i) &= \sum_{k=0}^{N} d_{ik}^{(n)} F(x_k) or \left\{F_{,x}^{(n)}\right\}_{(N+1)\times 1} \\ &= \left[D^{(n)}\right]_{(N+1)\times(N+1)} \{F\}_{(N+1)\times 1} \end{aligned} \tag{11}$$

where (N + 1) is the number of collocation points, F(n) ,x (xi) indicates nth differentiation of function F in ith collocation point and D(n) - is called the nth differentiation matrix whose components for the first derivative, D(1) - , based on Chebyshev basic functions are (Trefethen 2000):

$$d_{00}^{(1)} = \frac{2N^2+1}{6}, \; d_{NN}^{(1)} = -\frac{2N^2+1}{6}, \tag{12a}$$

$$d_{jj}^{(1)} = \frac{-x_j}{2\left(1-x_j^2\right)}, \; j = 1, \ldots, N-1, \tag{12b}$$

$$d_{ij}^{(1)} = \frac{c_i(-1)^{i+j}}{c_j\left(x_i - x_j\right)}, \; i \neq j, i, j = 0, \ldots, N, \tag{12c}$$

$$c_i = \begin{cases} 2 & i = 0 \text{ or N}, \\ 1 & \text{otherwise} \end{cases} \tag{12d}$$

The second differentiation matrix, D(2) - , can be easily computed as the square of D(1) - . Trefethen(2000) provides some explicit formulas for higher order differentiation matrices. The method could be extended to two-dimensional domains by explaining the nth partial derivative by use of Kronecker products as follows:

$$\left\{\frac{\partial^{(n)}F}{\partial x^{(n)}}\right\}_{(N+1)^2\times 1} = \left[\boldsymbol{D}^{(n)}\otimes \boldsymbol{I}\right]_{(N+1)^2\times(N+1)^2}\{F\}_{(N+1)^2\times 1}, \tag{13a}$$

$$\left\{\frac{\partial^{(m)}F}{\partial y^{(m)}}\right\}_{(N+1)^2\times 1} = \left[\boldsymbol{I}\otimes \boldsymbol{D}^{(m)}\right]_{(N+1)^2\times(N+1)^2}\{F\}_{(N+1)^2\times 1} \tag{13b}$$

$$\left\{\frac{\partial^{(n+m)}F}{\partial x^{(n)}\partial y^{(m)}}\right\}_{(N+1)^2\times 1} = \left[\boldsymbol{D}^{(n)}\otimes \boldsymbol{I}\right]_{(N+1)^2\times(N+1)^2} \left[\boldsymbol{I}\otimes \boldsymbol{D}^{(m)}\right]_{(N+1)^2\times(N+1)^2}\{F\}_{(N+1)^2\times 1} \tag{13c}$$

If A and B are two matrices of dimensions p × q and r × s, respectively, then the Kronecker product, A ⊗ B, is the matrix of dimension pr × qs with p × q block form, where the i,j block is aijB. Also, I denotes the (N + 1) × (N + 1) identity matrix (Trefethen 2000).

Chebyshev polynomials are orthogonal in the range of [−1, 1]. Therefore, the rectangular real domain of nano plate needs to be mapped to a 2 × 2 square computational domain by the following transformations (see Fig. 2).

$$\bar{x} = \frac{2x}{a} - 1,\ \bar{y} = \frac{2y}{b} - 1,\ \bar{x},\bar{y} \in [-1,1] \tag{14}$$

The grid points in both $\bar{x}$ and $\bar{y}$ directions are selected based on the Gauss–Lobatto interpolation points as follows to optimize the distribution (Boyd 2000):

$$\bar{x}_i = \cos\left(\frac{\pi i}{N}\right), \bar{y}_j = \cos\left(\frac{\pi j}{N}\right), \quad i,j = 0,1,2,\ldots,N \tag{15}$$

Also, the following dimensionless parameters are introduced to make the problem dimensionless.

$$\begin{aligned} &(\bar{w}_0,\bar{z}_0) = (w_0,z_0)/h,\ \alpha = h/a,\ \beta = h/b,\ \gamma = a/b,\\ &\bar{\mu} = \mu/a^2,\ \bar{t} = \frac{t}{h}\sqrt{A/I_0}\left(\bar{\omega} = \Omega h\sqrt{I_0/A}\right),\\ &\bar{m} = M_0/\rho hab, \bar{k} = K_0/A \end{aligned} \tag{16}$$

where Ω and $\bar{\omega}$ are the factual and dimensionless natural frequency of the system, respectively. For the purpose of frequency analysis, the dimensionless displacement components are considered as:

$$\bar{w}_0(\bar{x},\bar{y},\bar{t}) = \bar{w}(\bar{x},\bar{y})e^{i\bar{\omega}\bar{t}} \tag{17a}$$

$$\varphi_x(\bar{x},\bar{y},\bar{t}) = \bar{\varphi}_x(\bar{x},\bar{y})e^{i\bar{\omega}\bar{t}} \tag{17b}$$

$$\varphi_y(\bar{x},\bar{y},\bar{t}) = \bar{\varphi}_y(\bar{x},\bar{y})e^{i\bar{\omega}\bar{t}} \tag{17c}$$

$$\bar{z}_0(\bar{t}) = \bar{z}e^{i\bar{\omega}\bar{t}} \tag{17d}$$

Substituting Eqs. (14), (16) and (17a, 17b, c, d) into Eqs. (9a, b, c, d, e and 10a, b), the dimensionless eigenvalue problem for free vibration of nano plates with attached mass can be rewritten in the following form:

$$K_s\frac{(1-\nu)}{2}\left(4\alpha^2\bar{w}_{,\bar{x}\bar{x}}+4\beta^2\bar{w}_{,\bar{y}\bar{y}}+2\alpha\bar{\varphi}_{x,\bar{x}}+2\beta\bar{\varphi}_{y,\bar{y}}\right)$$
$$=-\bar{\omega}^2\left(\bar{w}-4\bar{\mu}\bar{w}_{,\bar{x}\bar{x}}-4\gamma^2\bar{\mu}\bar{w}_{,\bar{y}\bar{y}}\right) \tag{18a}$$

$$4\alpha^2\bar{\varphi}_{x,\bar{x}\bar{x}}+4\nu\alpha\beta\bar{\varphi}_{y,\bar{x}\bar{y}}+2(1-\nu)\left(\beta^2\bar{\varphi}_{x,\bar{y}\bar{y}}+\alpha\beta\bar{\varphi}_{y,\bar{x}\bar{y}}\right)$$
$$-6K_s(1-\nu)\left(\bar{\varphi}_x+2\alpha\bar{w}_{,\bar{x}}\right)$$
$$=-\bar{\omega}^2\left(\bar{\varphi}_x-4\bar{\mu}\bar{\varphi}_{x,\bar{x}\bar{x}}-4\gamma^2\bar{\mu}\bar{\varphi}_{x,\bar{y}\bar{y}}\right) \tag{18b}$$

$$4\beta^2\bar{\varphi}_{y,\bar{y}\bar{y}}+4\nu\alpha\beta\bar{\varphi}_{x,\bar{x}\bar{y}}+2(1-\nu)\left(\alpha^2\bar{\varphi}_{y,\bar{x}\bar{x}}+\alpha\beta\bar{\varphi}_{x,\bar{x}\bar{y}}\right)$$
$$-6K_s(1-\nu)\left(\bar{\varphi}_y+2\beta\bar{w}_{,\bar{y}}\right)$$
$$=-\bar{\omega}^2\left(\bar{\varphi}_y-4\bar{\mu}\bar{\varphi}_{y,\bar{x}\bar{x}}-4\gamma^2\bar{\mu}\bar{\varphi}_{y,\bar{y}\bar{y}}\right) \tag{18c}$$

$$\bar{k}[\bar{w}-\bar{z}]_{(x_0,y_0)}=-\bar{\omega}^2\frac{\bar{m}}{\alpha\beta}\bar{z} \tag{18d}$$

$$\int_{-1}^{1}\int_{-1}^{1}\left\{K_s\frac{(1-\nu)}{2}\left(4\alpha^2\bar{w}_{,\bar{x}\bar{x}}+4\beta^2\bar{w}_{,\bar{y}\bar{y}}+2\alpha\bar{\varphi}_{x,\bar{x}}+2\beta\bar{\varphi}_{y,\bar{y}}\right)\right.$$
$$\left.+\bar{\omega}^2\left(\bar{w}-4\bar{\mu}\bar{w}_{,\bar{x}\bar{x}}-4\gamma^2\bar{\mu}\bar{w}_{,\bar{y}\bar{y}}\right)\right\}d\bar{x}d\bar{y}=4\bar{k}\alpha\beta\left[\bar{w}(\bar{x}_0,\bar{y}_0)-\bar{z}\right] \tag{18e}$$

The dimensionless boundary conditions are

Clamped (CCCC):

$$At\bar{x}=-1,+1\ \ and\ \bar{y}=-1,+1:\bar{w}=0,\ \ \bar{\varphi}_x=0,\ \ \bar{\varphi}_y=0 \tag{19a}$$

Simply Supported (SSSS):

$$At\bar{x}=-1,+1:\bar{w}=0,\bar{\varphi}_y=0,\bar{\varphi}_{x,\bar{x}}=0$$
$$At\bar{y}=-1,+1:\bar{w}=0,\bar{\varphi}_x=0,\bar{\varphi}_{y,\bar{y}}=0 \tag{19b}$$

One can obtain the discrete form of equations based on the pseudo-spectral method by applying Eqs. (13a, b, c) to Eqs. (18a, b, c, d) and (19a, b)

$$K_s\frac{(1-\nu)}{2}\left(4\alpha^2\left(\boldsymbol{D}^{(2)}\otimes\boldsymbol{I}\right)\{\bar{w}\}+4\beta^2\left(\boldsymbol{I}\otimes\boldsymbol{D}^{(2)}\right)\{\bar{w}\}\right.$$
$$\left.+2\alpha\left(\boldsymbol{D}^{(1)}\otimes\boldsymbol{I}\right)\{\bar{\varphi}_x\}+2\beta\left(\boldsymbol{I}\otimes\boldsymbol{D}^{(1)}\right)\{\bar{\varphi}_y\}\right)$$
$$=-\bar{\omega}^2\left(\{\bar{w}\}-4\bar{\mu}\left(\boldsymbol{D}^{(2)}\otimes\boldsymbol{I}\right)\{\bar{w}\}\right.$$
$$\left.-4\gamma^2\bar{\mu}\left(\boldsymbol{I}\otimes\boldsymbol{D}^{(2)}\right)\{\bar{w}\}\right)4\alpha^2\left(\boldsymbol{D}^{(2)}\otimes\boldsymbol{I}\right)\{\bar{\varphi}_x\}$$
$$+4\nu\alpha\beta\left(\boldsymbol{D}^{(1)}\otimes\boldsymbol{I}\right)\left(\boldsymbol{I}\otimes\boldsymbol{D}^{(1)}\right)\{\bar{\varphi}_y\} \tag{20a}$$

$$
\begin{aligned}
&+2(1-\nu)\left(\beta^2\left(\boldsymbol{I}\otimes\boldsymbol{D}^{(2)}\right)\{\bar{\varphi}_x\}+\alpha\beta\left(\boldsymbol{D}^{(1)}\otimes\boldsymbol{I}\right)\left(\boldsymbol{I}\otimes\boldsymbol{D}^{(1)}\right)\{\bar{\varphi}_y\}\right)\\
&-6K_s(1-\nu)\left(\{\bar{\varphi}_x\}+2\alpha\left(\boldsymbol{D}^{(1)}\otimes\boldsymbol{I}\right)\{\bar{w}\}\right)\\
&=-\bar{\omega}^2\left(\{\bar{\varphi}_x\}-4\bar{\mu}\left(\boldsymbol{D}^{(2)}\otimes\boldsymbol{I}\right)\{\bar{\varphi}_x\}-4\gamma^2\bar{\mu}\left(\boldsymbol{I}\otimes\boldsymbol{D}^{(2)}\right)\{\bar{\varphi}_x\}\right)
\end{aligned}
\tag{20b}
$$

$$
\begin{aligned}
&4\beta^2\left(\boldsymbol{I}\otimes\boldsymbol{D}^{(2)}\right)\{\bar{\varphi}_y\}+4\nu\alpha\beta\left(\boldsymbol{D}^{(1)}\otimes\boldsymbol{I}\right)\left(\boldsymbol{I}\otimes\boldsymbol{D}^{(1)}\right)\{\bar{\varphi}_x\}\frac{1}{2}\\
&+2(1-\nu)\left(\alpha^2\left(\boldsymbol{D}^{(2)}\otimes\boldsymbol{I}\right)\{\bar{\varphi}_y\}+\alpha\beta\left(\boldsymbol{D}^{(1)}\otimes\boldsymbol{I}\right)\left(\boldsymbol{I}\otimes\boldsymbol{D}^{(1)}\right)\{\bar{\varphi}_x\}\right)\\
&-6K_s(1-\nu)\left(\{\bar{\varphi}_y\}+2\beta\left(\boldsymbol{I}\otimes\boldsymbol{D}^{(1)}\right)\{\bar{w}\}\right)\\
&=-\bar{\omega}^2\left(\{\bar{\varphi}_y\}-4\bar{\mu}\left(\boldsymbol{D}^{(2)}\otimes\boldsymbol{I}\right)\{\bar{\varphi}_y\}-4\gamma^2\bar{\mu}\left(\boldsymbol{I}\otimes\boldsymbol{D}^{(2)}\right)\{\bar{\varphi}_y\}\right)
\end{aligned}
\tag{20c}
$$

$$
\bar{k}[\bar{w}-\bar{z}]_{(x_0,y_0)}=-\bar{\omega}^2\frac{\bar{m}}{\alpha\beta}\bar{z} \tag{20d}
$$

where {w¯}, {ϕ¯x} and ϕ¯y - are the vectors of the dimension (N + 1) 2 × 1 which indicate dimensionless displacement components in the grid points. The spectral analogs of boundary conditions for simply supported boundaries can be expressed as:

$$
\begin{aligned}
&At\bar{x}=-1,+1:\left(\boldsymbol{D}^{(1)}\otimes\boldsymbol{I}\right)\{\bar{\varphi}_x\}=0\\
&At\bar{y}=-1,+1:\left(\boldsymbol{I}\otimes\boldsymbol{D}^{(1)}\right)\{\bar{\varphi}_y\}=0
\end{aligned}
\tag{21}
$$

The standard matrix form of the eigenvalue problem of Eqs. (20a, b, c, d) and (21) could be presented as follows:

$$
\left(\left[\tilde{K}\right]+\bar{\omega}^2[M]\right)\begin{Bmatrix}\{\bar{w}\}\\\{\bar{\varphi}_x\}\\\{\bar{\varphi}_y\}\\\bar{z}\end{Bmatrix}=\{0\} \tag{22}
$$

Equation (22), which represents the discrete governing equations of motion, is valid in all the grid points except than kth grid point where the mass-spring system is located, due to the singularity of the lateral governing equation in this point. Therefore, the lateral governing equation in kth grid point needs to be replaced with the integral Eq. (18e) as it will be explained in the next section.

4. Integral quadrature procedure

In integral quadrature (IQ) method, the main idea is to evaluate the integration of an arbitrary function, H, on a domain by an equivalent weighted linear sum of the function values at all collocation points of the domain (Eftekhari and Jafari 2012). The IQ method for the present two-dimensional computational domain (Fig. 2) can be written as:

$$
\int_{-1}^{+1}\int_{-1}^{+1}H(\bar{x},\bar{y})d\bar{x}d\bar{y}=\sum_{i=1}^{(N+1)^2}l_iH_i=[L]_{1\times(N+1)^2}\{R\}_{(N+1)^2\times1} \tag{23}
$$

For applying the method, it is necessary to determine the associated weighting coefficients, li. It can be simply performed by introducing a set of (N + 1) 2 polynomial test functions as follows (Eftekhari and Jafari 2012):

$$H_t = x^m y^n,\ m,n = 0,\ldots,N \tag{24}$$

As the values of these polynomials are known in the grid points and the values of their integrals on the domain can be easily computed, the weighting coefficients matrix, [L], will be simply evaluated through an inverse problem.

Here, the IQ method will be implemented to discrete the integral form of the lateral governing equation of motion, Eq. (18e), as follows:

$$\begin{aligned}&[L]\left[K_s\frac{(1-\nu)}{2}\left(4\alpha^2\left(\boldsymbol{D}^{(2)}\otimes\boldsymbol{I}\right)\{\bar{w}\}+4\beta^2\left(\boldsymbol{I}\otimes\boldsymbol{D}^{(2)}\right)\{\bar{w}\}+2\alpha\left(\boldsymbol{D}^{(1)}\otimes\boldsymbol{I}\right)\{\bar{\varphi}_x\}+2\beta\left(\boldsymbol{I}\otimes\boldsymbol{D}^{(1)}\right)\right.\right.\\&\left.\left.\{\bar{\varphi}_y\}\right)+\bar{\omega}^2\left(\{\bar{w}\}-4\bar{\mu}\left(\boldsymbol{D}^{(2)}\otimes\boldsymbol{I}\right)\{\bar{w}\}-4\gamma^2\bar{\mu}\left(\boldsymbol{I}\otimes\boldsymbol{D}^{(2)}\right)\{\bar{w}\}\right)\right]=4\bar{k}\alpha\beta\left[\bar{w}(\bar{x}_0,\bar{y}_0)-\bar{z}\right]\end{aligned} \tag{25}$$

Now, the singular lateral governing equation in kth grid point in Eq. (22) could be replaced with Eq. (25) as the following matrix form:

$$\left[\hat{I}\right]\left[\left(\left[\tilde{K}\right]+\bar{\omega}^2[M]\right)\begin{Bmatrix}\{\bar{w}\}\\\{\bar{\varphi}_x\}\\\{\bar{\varphi}_y\}\\\bar{z}\end{Bmatrix}\right]=\left[\hat{K}\right]\begin{Bmatrix}\{\bar{w}\}\\\{\bar{\varphi}_x\}\\\{\bar{\varphi}_y\}\\\bar{z}\end{Bmatrix} \tag{26a}$$

where

$$\hat{I}_{ij}=\begin{cases}1 & i=j, i\neq k\\ l_j & i=k\\ 0 & \text{otherwise}\end{cases} \tag{26b}$$

Components of Kˆ - are equal to zero except than two components in kth row which contains terms from the right hand of Eq. (25). Due to the simple form of matrices ˆI - and Kˆ - , Eq. (26a) can be rewritten in the following form:

$$\left([K]+\bar{\omega}^2[M]\right)\begin{Bmatrix}\{\bar{w}\}\\\{\bar{\varphi}_x\}\\\{\bar{\varphi}_y\}\\\bar{z}\end{Bmatrix}=\{0\} \tag{27a}$$

where

$$\begin{aligned}&[K]=\left[\tilde{K}\right]+\left[K^*\right]\\&\left[K^*\right]=\left[\hat{I}\right]^{-1}\left[\hat{K}\right]=\left[\hat{K}\right]/l_k\end{aligned} \tag{27b}$$

To establish the standard eigenvalue form of the problem, the displacement vectors can be divided to the boundary and the domain parts as follows.

$$\begin{Bmatrix}\bar{w}_b\\\bar{\varphi}_{xb}\\\bar{\varphi}_{yb}\end{Bmatrix}=\{b\},\begin{Bmatrix}\bar{w}_d\\\bar{\varphi}_{xd}\\\bar{\varphi}_{yd}\\\bar{z}\end{Bmatrix}=\{d\} \tag{28}$$

where the subscripts b and d indicate boundary and domain, respectively. Then, the resulting eigenvalue of equations can be written in the matrix form as:

$$\left(\begin{bmatrix} K_{bb} & K_{bd} \\ K_{db} & K_{dd} \end{bmatrix} + \bar{\omega}^2 \begin{bmatrix} 0 & 0 \\ M_{db} & M_{dd} \end{bmatrix}\right) \begin{Bmatrix} b \\ d \end{Bmatrix} = 0 \tag{29a}$$

$$[K_{bb}]\{b\} + [K_{bd}]\{d\} = 0, \tag{29b}$$

$$[K_{db}]\{b\} + [K_{dd}]\{d\} = -\bar{\omega}^2([M_{db}]\{b\} + [M_{dd}]\{d\}) \tag{29c}$$

Eliminating the boundary displacement vector, {b}, from Eq. (29a, 29b, 29c) one obtains

$$\left([\bar{K}] + \bar{\omega}^2[\bar{M}]\right)\{d\} = 0 \tag{30a}$$

$$[\bar{K}] = [K_{dd}] - [K_{db}][K_{bb}]^{-1}[K_{bd}], \tag{30b}$$

$$[\bar{M}] = [M_{dd}] - [M_{db}][K_{bb}]^{-1}[K_{bd}] \tag{30c}$$

where $\bar{K}$ - and $\bar{M}$ - are the total stiffness and mass matrices, respectively.

5. Results and discussion

At first, the validation and convergence study is done to be sure about the reliability and accuracy of the solution procedure. Table 1 lists the fundamental frequency of a bare nano plate without any attached mass-spring system for various values of small scale parameter, length size, and aspect ratio. An excellent agreement with the exact results of nonlocal FSDT plate model by Pradhan and Phadikar (2009) is observed that confirms the competence of the present method. Also, an admissible convergence is obtained with N = 8 grid points which is used for all the next results.

Influence of attached mass-spring system on frequency response of the plate is presented in Table 2 and results are compared with exact results by Avalos et al. (1993). For possibility of comparison, small scale parameter, μ, is considered equal to zero and thickness to length size ratio is set to α = 0.001, as the result by Avalos et al. (1993) are presented for a thin macro plate. The desirable match between present and exact results proves the accuracy and efficiency of combined pseudo-spectral and IQ approach in prediction of vibrational characteristic of systems with concentrated objects.

In following, the frequency response of a nano plate carrying a mass-spring system is presented and influence of spring constant, small scale parameter, boundary conditions, thickness to side ratio, aspect ratio, and mass location on the frequency response as a resonant mass sensor is discussed in detail. Since graphene is most famous nano structure with a plane shape and its potential application as a resonant mass sensor is addressed in many recent researches, the material properties of nano plate in coming results are considered equal to a graphene sheet with Young's modulus E = 1.06 TPa, Poisson's ratio v = 0.16, density ρ = 2250 kg/m3 , and effective thickness h = 0.34 nm (Kitipornchai et al. 2005).

The potential application of a nano plate as a resonant sensor for detecting attached masses is related to its frequency shift, Δf, due to changes in the value of attached mass. Frequency shift is defined as the difference between fundamental frequency of a nano plate with attached mass and fundamental frequency of a bare nano plate, f0, and dimensionless frequency shift is indicated as Δf/f0. In order to investigate the influence of elastic connection between the nano plate and the attached mass, Fig. 3 shows variation of Δf/f0 versus variation of dimensionless spring constant, $\bar{k}$ for different values of thickness to side ratio, α. An attached mass of $\bar{m}$ = 0.5 at the center of a simply supported square nano plate with $\bar{\mu}$ = 0.01 is considered. It is shown that for soft connections

with small values of spring constant the frequency shift has its maximum value while increasing the rigidity of connection decreases the frequency shift to an ultimate frequency shift of a fully rigid connection. It means that considering a rigid connection instead of an elastic one will underestimate the frequency shift of nano resonant sensors. It should be noted that for very small spring constants, the connection between the nano plate and the attached mass is not strong enough to allow them to vibrate together having a mode shape corresponds to the first mode shape of a bare plate, but with a smaller frequency. Hence, the minimum value of $\bar{k} = 0.05$ is considered in presented results. Although increasing thickness to side ratio decreases dimensionless frequency of nano plate due to shear deformation effects (Reddy 2003), however from Fig. 3 one can see that increasing thickness to side ratio increases dimensionless frequency shift for especially for soft connections. For a nano plate with a specified thickness, like graphene sheets with h = 0.34 nm, it means smaller sheets present higher value of Δf/f0 for a certain spring constant.

Figure 4 depicts the variation of dimensionless frequency shift, Δf/f0 with respect to dimensionless nonlocal small scale parameter, $\bar{\mu}$, for various values of dimensionless mass. Results are presented for a simply supported square nano plate with an attached mass-spring system in its center. It is observed that for every value of attached mass and spring constant, increasing nonlocal parameter causes a decrease in Δf/f0. It can be concluded that neglecting the nonlocal small scale effect results in overestimating the capability of nano plates in resonant sensing applications. Two values of spring constant is considered in the presented results. From the plots in Fig. 3, for a nano plate with $\alpha = 0.03$ the spring constant of $\bar{k} = 0.05$ is considered for a soft connection while $\bar{k} = 0.30$ is selected to represent an almost rigid connection. As it is expected soft connections propose greater frequency shifts for every value of the dimensionless nonlocal parameter and the attached mass.

Figure 5a demonstrates variation of dimensionless frequency shift versus dimensionless attached mass for different values of dimensionless nonlocal parameter. Results are plotted for a simply supported square nano plate with $\alpha = 0.03$ and a mass-spring attached in its center. It is obvious that when the value of attached mass increases the frequency shift of nano plate increases. Indeed, it is the way to determine the value of mass by measuring the value of frequency shift. However, as it was observed in Fig. 4 for a constant value of attached mass, increasing the nonlocal parameter causes a decrease in frequency shift. It means nano plates with higher degree of discontinuity have less capability to detect attached particles. Dimensionless sensitivity, S, is defined as the partial derivative of dimensionless frequency shift with respect to dimensionless mass, $\partial(\bar{f}/f0)/\partial(\bar{m})$. Figure 5b depicts dimensionless sensitivity of nano plates as the slope of Fig. 5a. In general, sensitivity increases when the dimensionless mass decreases and the maximum sensitivity is achieved when the mass tends to zero. Sensitivity decreases dramatically when the attached mass tends to the value as great as the nano plate mass ($\bar{m} = 1$), which means nano plates are not much sensitive to the changes of the value of attached mass for such heavy masses.

Boundary conditions can significantly affect the frequency shift. As it is expected, clamped boundaries present higher dimensionless frequency shift than simply supported ones due to increasing total stiffness of the system. Table 3 lists the percent of enhancing of dimensionless frequency shift due to changing boundary conditions from simply supported to clamped boundaries. It is seen that when the dimensionless nonlocal parameter increases the enhancing effect of clamped boundaries increases. Also, nano plates with clamped boundaries present greater enhancing effect when the dimensionless attached mass is smaller. In order to explore the influence of aspect ratio, γ, variation of dimensionless frequency shift versus aspect ratio for various values of spring constant is shown in Fig. 6. An attached mass of $\bar{m} = 0.5$ at the center of a simply supported nano plate with $\bar{\mu} = 0.01$ and $\alpha = 0.03$ is considered. Results reveal that increasing aspect ratio decreases the frequency shift which means for a specified thickness to side ratio, nano plates with longer rectangular shapes have less dimensionless frequency shift and the maximum belongs to square nano plates. Also, it is shown that soft connections between nano plates and the attached mass propose greater frequency shifts especially for rectangular plates with great aspect ratios.

The position of attached mass is also a significant issue. Figure 7 gives the influence of the attached mass-spring position on dimensionless frequency shift of a square nano plate with $\bar{\mu} = 0.01$ carrying an attached mass of $\bar{m} = 0.5$. Although the absolute maximum frequency shift occurs when the mass is exactly located at the center of plate, for a central area equals to 25 % of the total sensing surface, the frequency shifts are at least 70 % of the absolute maximum value. The frequency shifts decrease dramatically by approaching the boundaries. Hence, in particular it is recommended to locate the measured object as near as the center of resonant sensor.

This work aims to parametrically investigate the influence of geometric parameters and material properties of a planar nanostructure on its potential application as a resonant mass sensor. The aforementioned results may be used as a general guideline for designing future such nano resonant sensors. Hence, all provided results are dimensionless to keep the generality and possibility of application for various planar nano sensors. However, it should be noted that based on selected nanostructure as resonant sensor and specifying the object nano particle, all the geometric and material properties can be obtained and the presented dimensionless results can be utilized. For instance, an SLGS with a proper surface area may be selected to detect metallic nanoparticles. In this case, all the geometric parameters and material properties of graphene are specified and the spring constant is considered to represent atomic forces between carbon atoms of SLGSs and the attached metallic particle.

6. Conclusion

In the present study, the potential application of nano plates as nano resonant mass sensors is investigated by introducing a nonlocal shear deformation plate model with an elastically mounted attached mass. A combination of pseudospectral and integral quadrature methods is implemented to numerically determine the frequency shift caused by attached mass-spring system. Influence of several dimensionless parameters like small scale parameter, spring constant, thickness to side ratio, aspect ratio, mass location and boundary conditions on the frequency shift is discussed in detail and the conclusions are listed as follows.

• The validation study approves that the proposed combined numerical method can be implemented to solve structural problems with concentrated objects.

• Increasing the spring constant results in lower values of frequency shift. Therefore, it can be conclude that considering rigid connection instead of elastic one will underestimate the frequency shift of nano resonant sensor.

• Nano plates with greater aspect ratios offer lower dimensionless frequency shifts and the maximum is related to a square one. Also, increasing thickness to side ratio increases dimensionless frequency shifts.

• Nano plates with clamped boundary conditions present greater dimensionless frequency shift in comparison to simply supported ones, especially when the dimensionless attached mass is smaller.

• Increasing the small scale parameter causes a decrease in frequency shift. It means neglecting nonlocal small scale parameter results in overestimating the frequency shift of nano resonant sensors.

• Increasing the value of attached mass as well as closing it to the center of plate increase the frequency shift.

Acknowledgements

Pugno NM is supported by the European Research Council (ERC StG Ideas 2011 BIHSNAM on “Bio-Inspired hierarchical super-nanomaterials”, ERC PoC 2013-1 REPLICA2 on “Large-area replication of biological anti-adhesive nanosurfaces”, ERC PoC2013-2 KNOTOUGH on “Super-tough knotted fibres”) and European Commission under Graphene Flagship.

References

Adhikari S, Chowdhury R (2012) Zeptogram sensing from gigahertz vibration: graphene based nanosensor. Physica E 44:1528–1534

Angione MD et al (2014) Carbon based materials for electronic biosensing. Mater Today 14(9):424–433

Ansari R, Ajori S, Arash B (2012) Vibrations of single- and doublewalled carbon nanotubes with layerwise boundary conditions: a molecular dynamics study. Curr Appl Phys 12:707–711

Arash B, Wang Q (2012) A review on the application of nonlocal elastic models in modeling of carbon nanotubes and graphenes. Comp Mater Sci 51:303–313

Arash B, Wang Q, Duan WH (2011) Detection of gas atoms via vibration of graphenes. Phys Lett A 375:2411–2415

Avalos DR, Larrondo H, Laurat PAA (1993) Vibrations of a simply supported plate carrying an elastically mounted concentrated mass. Ocean Eng 20(2):195–205

Behfar K, Naghdabadi R (2005) Nanoscale vibrational analysis of a multi-layered graphene sheet embedded in an elastic medium. Compos Sci Technol 65:1159–1164

Boyd JP (2000) Chebyshev and fourier spectral methods. Dover, New York

Eftekhari SA, Jafari AA (2012) Vibration of an initially stressed rectangular plate due to an accelerated traveling mass. Sci Iran A 19(5):1195–1213

Eringen AC (1983) On differential equations of nonlocal elasticity and solutions of screw dislocation and surface waves. J Appl Phys 54:4703–4710

Eringen AC (2002) Nonlocal continuum field theories. Springer, NY

Giannopoulos GI (2014) Fullerenes as mass sensors: a numerical investigation. Physica E 56:36–42

Jalali SK, Naei MH, Poorsolhjouy A (2010) Thermal stability analysis of circular functionally graded sandwich plates of variable thickness using pseudo-spectral method. Mater Design 31:4755–4763

Jalali SK, Naei MH, Poorsolhjouy A (2011) Buckling of circular sandwich plates of variable core thickness and FGM face sheets. Int J Struct Stab Dy 11(2):273–295

Jalali SK, Naei MH, Pugno NM (2014) Graphene-based resonant sensors for detection of ultra-fine nanoparticles: molecular dynamics and nonlocal elasticity investigations. Nano. doi:10.1142/S1793292015500241

Jomehzadeh E, Saidi AR, Pugno NM (2012) Large amplitude vibration of a bilayer graphene embedded in a nonlinear polymer matrix. Physica E 44:1973–1982

Joshi AY, Harsha SP, Sharma SC (2010) Vibration signature analysis of single walled carbon nanotube based nanomechanical sensors. Physica E 42:2115–2123

Kitipornchai S, He XQ, Liew KM (2005) Continuum model for the vibration of multilayered graphene sheets. Phys Rev B 72:075443

Lee HL, Yang YC, Chang WJ (2013a) Mass detection using a graphene-based nanomechanical resonator. Jpn J Appl Phys 52:025101

Lee HL, Hsu JC, Lin SY, Chang WJ (2013b) Sensitivity analysis of single-layer graphene resonators using atomic finite element method. J Appl Phys 114:123506

Liew KM, He XQ, Kitipornchai S (2006) Predicting nanovibration of multi-layered graphene sheets embedded in an elastic matrix. Acta Mater 54:4229–4236

Mehdipour I, Barari A, Domairry G (2011) Application of a cantilevered SWCNT with mass at the tip as a nanomechanical sensor. Comp Mater Sci 50:1830–1833

Murmu T, Adhikari S (2013) Nonlocal mass nanosensors based on vibrating monolayer graphene sheets. Sensors Actuators B 188:1319–1327

Pradhan SC, Phadikar JK (2009) Nonlocal elasticity theory for vibration of nanoplates. J Sound Vib 325:206–223

Reddy JN (2003) Mechanics of laminated composite plates and shells: theory and analysis, 2nd edn. CRC Press, NY

Reddy JN (2008) An introduction to continuum mechanics. Cambridge University Press, NY

Sakhaee-Pour A (2009) Elastic buckling of single-layered graphene sheet. Comp Mater Sci 45:266–270

Sakhaee-Pour A, Ahmadian MT, Vafai A (2008) Applications of single-layered graphene sheets as mass sensors and atomistic dust detectors. Solid State Commun 145:168–172

Shen ZB, Tang HL, Li DK, Tang GJ (2012) Vibration of single-layered graphene sheet-based nanomechanical sensor via nonlocal Kirchhoff plate theory. Comp Mater Sci 61:200–205 Trefethen LN (2000) Spectral methods in matlab. SIAM, Philadelphia

Wang CG, Lan L, Liu YP, Tan HF, He XD (2013) Vibration characteristics of wrinkled single-layered graphene sheets. Int J Solids Struct 50:1812–1823

Xiang Y, Shen HS (2014) Tension buckling of graphene: a new phenotype. Solid State Commun 192:20–23

Zenkour AM, Abouelregal AE (2014) Nonlocal thermoelastic nanobeam subjected to a sinusoidal pulse heating and temperaturedependent physical properties. Microsyst Technol. doi:10.1007/ s00542-014-2294-5

Zhou SM, Sheng LP, Shen ZB (2014) Transverse vibration of circular graphene sheet-based mass sensor via nonlocal Kirchhoff plate theory. Comp Mater Sci 86:73–78

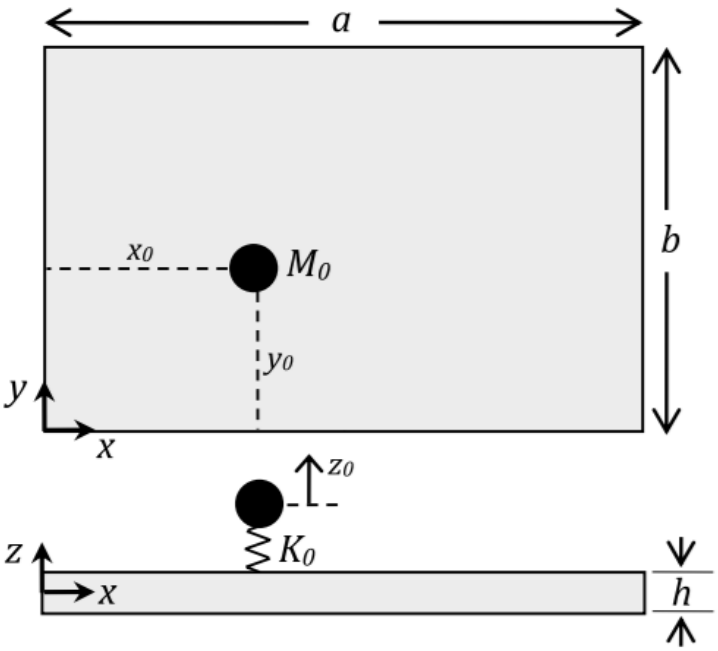

Fig. 1 Schematic of the studied nano plate with an attached mass-spring system

Fig. 2 Real and computational domains

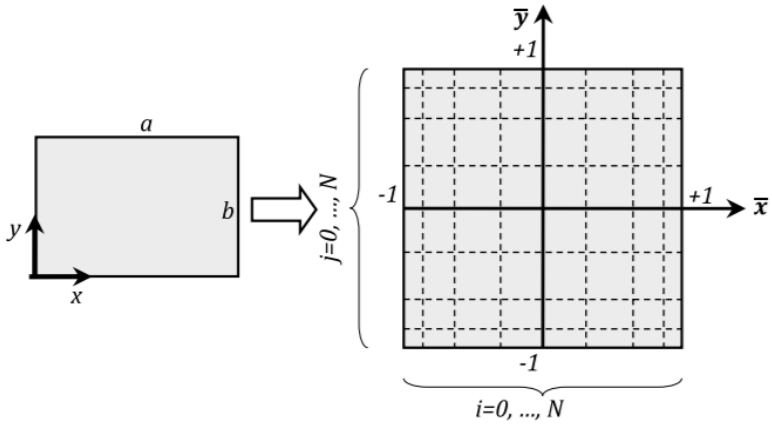

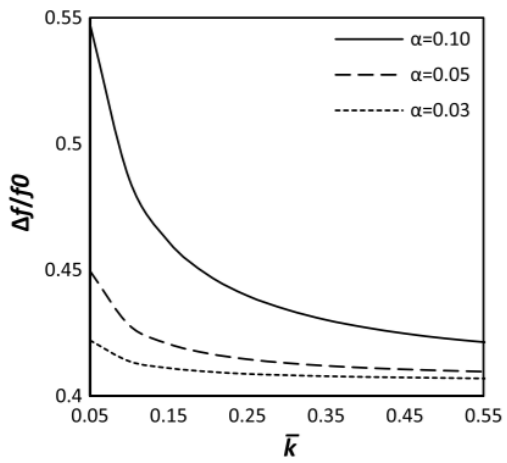

Fig. 3 Dimensionless frequency shift versus dimensionless spring constant for various values of thickness to side ratios ($\bar{\mu} = 0.01, \bar{m} = 0.5, \gamma = 1, \bar{x}_0 = \bar{y}_0 = 0, B.C. : SSSS$)

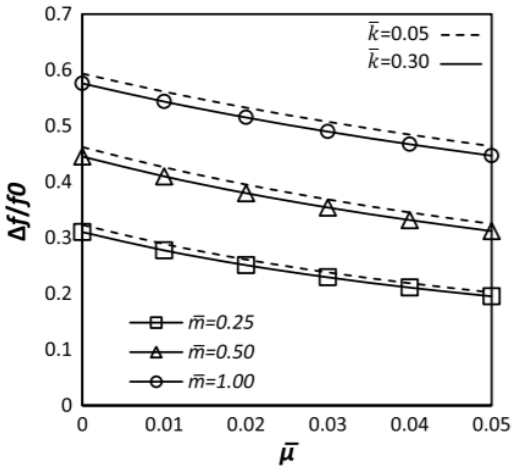

Fig. 4 Dimensionless frequency shift versus dimensionless nonlocal small scale parameter for various values of dimensionless attached mass and spring constant ($\alpha = 0.03, \gamma = 1, \bar{x}_0 = \bar{y}_0 = 0, B.C. : SSSS$)

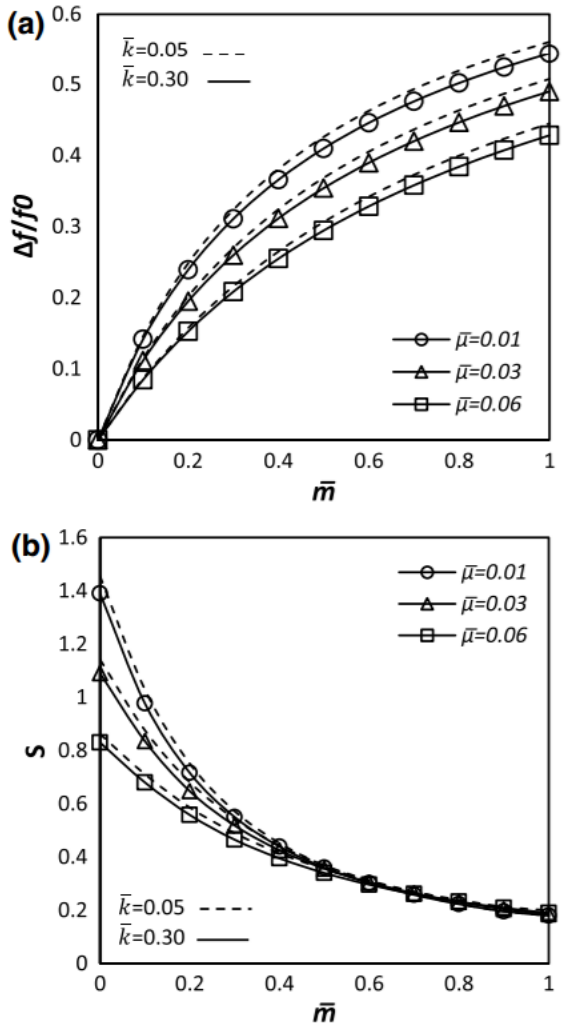

Fig. 5 **a** Dimensionless frequency shift, **b** dimensionless sensitivity, versus dimensionless attached mass for various values of dimensionless nonlocal small scale parameter and spring constant ($\alpha = 0.03,\ \gamma = 1,\ \bar{x}_0 = \bar{y}_0 = 0,\ B.C. : SSSS$)

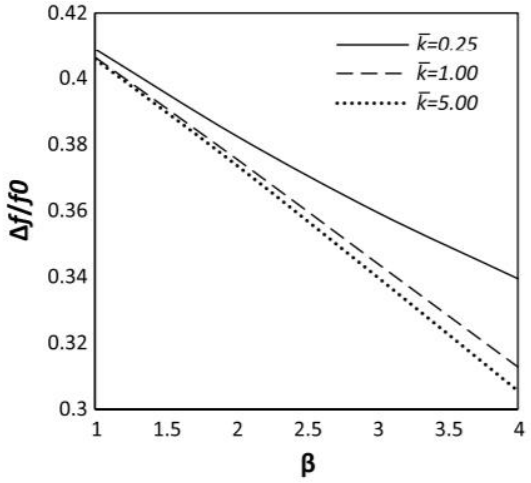

Fig. 6 Dimensionless frequency shift versus aspect ratio for various values of spring constant ($\alpha = 0.03, \bar{\mu} = 0.01, \bar{m} = 0.5, \bar{x}_0 = \bar{y}_0 = 0$, $B.C. : SSSS$)

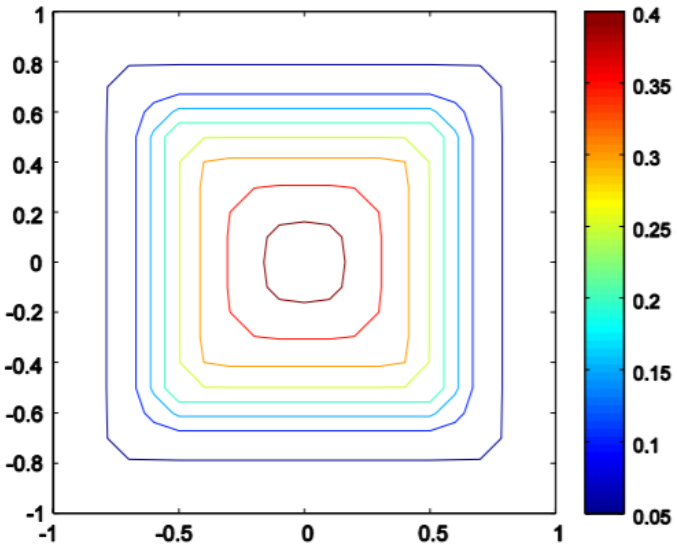

Fig. 7 .

Table 1 Convergence study of fundamental frequencies (THz) of simply supported nano plates. ($E = 1.06\,\text{Tpa}, \rho = 2250\,\text{kg/m}^3,$) ($\nu = 0.16, h = 0.34\,\text{nm}$)

γ	a(nm)	e_0a_0(nm)	$N = 5$	$N = 8$	$N = 10$	Pradhan and Phadikar (2009)	Error %
0.5	2.5	0	0.6319	0.6359	0.6359	0.6385	0.408
		1	0.3666	0.3688	0.3688	0.3703	0.406
		2	0.2120	0.2132	0.2132	0.2141	0.422
		3	0.1460	0.1468	0.1468	0.1474	0.408
	10	0	0.0406	0.0411	0.0411	0.0409	0.486
		1	0.0383	0.0387	0.0387	0.0386	0.258
		2	0.0333	0.0336	0.0336	0.0335	0.297
		3	0.0280	0.0283	0.0283	0.0282	0.353
1	2.5	0	0.9933	0.9978	0.9978	1.0062	0.841
		1	0.4873	0.4893	0.4893	0.4934	0.837
		2	0.2692	0.2703	0.2703	0.2725	0.813
		3	0.1832	0.1840	0.1840	0.1855	0.815
	10	0	0.0651	0.0656	0.0656	0.0654	0.304
		1	0.0595	0.0600	0.0600	0.0598	0.333
		2	0.0487	0.0490	0.0490	0.0489	0.204
		3	0.0391	0.0394	0.0394	0.0392	0.507

Table 2 Dimensionless frequency, $\hat{\omega} = \Omega a^2 \sqrt{I_0/D} = 2\sqrt{3}\bar{\omega}/\alpha^2$, of a square SSSS plate with elastically mounted spring-mass system at its center ($\nu = 0.3, \alpha = 0.001$)

$\bar{k}$	$\bar{m}$	First mode		Second mode	
		Present	Avalos et al. (1993)	Present	Avalos et al. (1993)
0.2	0.1	1.4126	1.41259	19.7600	19.75956
	1.0	0.4467	0.44670	19.7599	19.75947
	2.0	0.3159	0.31587	19.7599	19.75946
	5.0	0.1998	0.19977	19.7599	19.75946
1.0	0.1	3.1437	3.14395	19.8450	19.84277
	1.0	0.9942	1.00000	19.8437	19.84041
	2.0	0.7030	0.70310	19.8436	19.84028
	5.0	0.4446	0.44468	19.8436	19.84020
5.0	0.1	6.8514	6.85454	20.3224	20.30377
	1.0	2.1734	2.17417	20.2588	20.24257
	2.0	1.5370	1.53760	20.2559	20.23954
	5.0	0.9722	1.00000	20.2542	20.23773

Table 3 Percent of increase (%) of dimensionless frequency shift ($\Delta f / f_0$) due to changing boundary conditions from SSSS to CCCC

$\bar{m}$	$\bar{k}$	$\bar{\mu}$			
		0.00	0.01	0.03	0.06
0.3	0.05	28.97	29.49	30.08	30.34
	0.25	23.98	24.14	24.27	24.39
0.5	0.05	22.12	22.92	24.21	25.53
	0.25	18.58	18.94	19.52	20.25
1.0	0.05	14.71	15.41	16.69	18.35
	0.25	12.60	12.97	13.64	14.55